

Bounds on isocurvature perturbations from CMB and LSS data

Patrick Crotty,¹ Juan García-Bellido,² Julien Lesgourgues,^{1,3} and Alain Riazuelo⁴

¹*Laboratoire de Physique Théorique LAPTH, F-74941 Annecy-le-Vieux Cedex, France*

²*Departamento de Física Teórica C-XI, Universidad Autónoma de Madrid, Cantoblanco, 28049 Madrid, Spain*

³*TH-Division CERN, CH-1211 Gèneve 23, Switzerland*

⁴*Service de Physique Théorique CNRS, CEA/Saclay F-91191, Gif-sur-Yvette Cedex, France*

(Dated: May 22, 2019)

We obtain very stringent bounds on the possible cold dark matter, baryon and neutrino isocurvature contributions to the primordial fluctuations in the Universe, using recent cosmic microwave background and large scale structure data. In particular, we include the measured temperature and polarization power spectra from WMAP and ACBAR, as well as the matter power spectrum from the 2dF galaxy redshift survey. Neglecting the possible effects of spatial curvature, tensor perturbations and reionization, we perform a Bayesian likelihood analysis with nine free parameters, and find that the amplitude of the isocurvature component cannot be larger than about 31% for the cold dark matter mode, 91% for the baryon mode, 76% for the neutrino density mode, and 60% for the neutrino velocity mode, at 2σ , for uncorrelated models. On the other hand, for correlated adiabatic and isocurvature components, the fraction could be slightly larger. However, the cross-correlation coefficient is strongly constrained, and maximally correlated/anticorrelated models are disfavored. This puts strong bounds on the curvaton model, independently of the bounds on non-Gaussianity.

PACS numbers: 98.80.Cq

Preprint LAPTH-985/03, SPhT-T03/076, IFT-UAM/CSIC-03-19, CERN-TH/2003-124, astro-ph/0306286

Introduction. Thanks to the tremendous developments in observational cosmology during the last few years, it is possible to speak today of a Standard Model of Cosmology, whose parameters are known within systematic errors of just a few percent. Moreover, the recent measurements of both temperature and polarization anisotropies in the cosmic microwave background (CMB) has opened the possibility to test not only the basic paradigm for the origin of structure, namely inflation, but also the precise nature of the primordial fluctuations that gave rise to the CMB anisotropies and the density perturbations responsible for the large scale structure (LSS) of the Universe.

The simplest realizations of the inflationary paradigm predict an approximately scale invariant spectrum of adiabatic and Gaussian curvature fluctuations, whose amplitude remains constant outside the horizon, and therefore allows cosmologists to probe the physics of inflation through observations of the CMB anisotropies and the LSS matter distribution. However, this is by no means the only possibility. Multiple-field inflation predicts that, together with the adiabatic component, there should also be an entropy or isocurvature perturbation [1, 2, 3], associated with fluctuations in number density between different components of the plasma before decoupling, with a possible statistical correlation between the adiabatic and isocurvature modes [4]. Baryon and cold dark matter (CDM) isocurvature perturbations were proposed long ago [5] as an alternative to adiabatic perturbations. Recently, two other modes, neutrino isocurvature density and velocity perturbations, have been added to the list [6]. Topological defects also predict a significant isocurvature component. Moreover, it is well known that entropy perturbations seed curvature perturbations outside the horizon [2, 3], so it is possible that a signifi-

cant component of the observed adiabatic mode could be strongly correlated with an isocurvature mode. Such models are generically called *curvaton models* [7], and are now widely studied as an alternative to the standard paradigm. Furthermore, isocurvature modes typically induce non-Gaussian signatures in the spectrum of primordial perturbations.

In this Letter we present very stringent bounds on the various isocurvature components, coming from the temperature power spectrum and temperature-polarization cross-correlation recently measured by the WMAP satellite [8]; from the small-scale temperature anisotropy probed by ACBAR [9]; and from the matter power spectrum measured by the 2-degree-Field Galaxy Redshift Survey (2dFGRS) [10]. We do not use the data from Lyman- α forests, since they are based on non-linear simulations carried under the assumption of adiabaticity. We will not assume any specific model of inflation, or any particular mechanism to generate the perturbations (late decays, phase transitions, cosmic defects, etc.), and thus will allow all five modes – adiabatic (AD), baryon isocurvature (BI), CDM isocurvature (CDI), neutrino isocurvature density (NID) and neutrino isocurvature velocity (NIV) – to be correlated (or not) among each other, and to have arbitrary tilts. However, we will only consider the mixing of the adiabatic mode and one of the isocurvature modes at a time. This choice has the advantage of restricting considerably the parameter space, and reflects the fact that most of the proposed mechanisms for the generation of isocurvature perturbations lead to only one mode. The first bounds on isocurvature perturbations assumed uncorrelated modes [11], but recently also correlated ones were considered in Refs. [12, 13, 14, 15].

The present analysis neglects the possible effects of spatial curvature, tensor perturbations and reionization.

Therefore, each model is described by nine parameters: the cosmological constant Ω_Λ , the baryon density $\omega_B = \Omega_B h^2$, the cold dark matter density $\omega_{\text{cdm}} = \Omega_{\text{cdm}} h^2$, the overall normalisation A , the isocurvature mode relative amplitude α and correlation β , the adiabatic and isocurvature tilts (n_{ad} , n_{iso}), and finally a free bias b associated to the 2dF power spectrum. We generate a 5-dimensional grid of models (A , α , β , and b are not discretized) and perform of Bayesian analysis in the full 9-dimensional parameter space. At each grid point, we store some C_l values in the range $0 < l < 1800$ and some $P(k)$ values in the range probed by the 2dF data. The likelihood of each model is then computed using the software or the detailed information provided on the experimental websites, using 1398 points from WMAP, 11 points from ACBAR and 32 points from the 2dFGRS. For parameter values which do not coincide with grid points, our code first performs a cubic interpolation of each power spectrum, accurate to better than one percent, and then computes the likelihood of the corresponding model. From the limitation of our grid, we impose a flat prior on the isocurvature tilt: $n_{\text{iso}} > 0.6$ (inflation predicts the tilts to be close to one). The other grid ranges are wide enough in order not to affect our results.

For the theoretical analysis, we will use the notation and some of the approximations of Ref. [13]. For instance, the power spectra of adiabatic and isocurvature perturbations, as well as their cross-correlation, are parametrized with 3 power laws, i.e. three amplitudes and two spectral indices,

$$\begin{aligned} \Delta_{\mathcal{R}}^2(k) &\equiv \frac{k^3}{2\pi^2} \langle \mathcal{R}^2 \rangle = \mathcal{A}^2 \left(\frac{k}{k_0} \right)^{n_{\text{ad}}-1}, \\ \Delta_{\mathcal{S}}^2(k) &\equiv \frac{k^3}{2\pi^2} \langle \mathcal{S}^2 \rangle = \mathcal{B}^2 \left(\frac{k}{k_0} \right)^{n_{\text{iso}}-1}, \\ \Delta_{\mathcal{R}\mathcal{S}}^2(k) &\equiv \frac{k^3}{2\pi^2} \langle \mathcal{R}\mathcal{S} \rangle = \mathcal{A}\mathcal{B} \cos \Delta \left(\frac{k}{k_0} \right)^{(n_{\text{ad}}+n_{\text{iso}})/2-1}. \end{aligned} \quad (1)$$

where k_0 is an arbitrary pivot scale. We also assume that the correlation coefficient $\cos \Delta$ is scale-independent (Note that in Ref. [15] this assumption was relaxed). In order to evaluate the temperature and polarization anisotropies, one has to calculate the radiation transfer functions for adiabatic and isocurvature perturbations and compute the total angular power spectrum as [13]

$$C_l = C_l^{\text{ad}} + B^2 C_l^{\text{iso}} + 2B \cos \Delta C_l^{\text{corr}}, \quad (2)$$

where B is the entropy to curvature perturbation ratio during radiation domination, $B = \mathcal{S}/\mathcal{R}$. We will use here a slightly different notation, used before by other groups [4, 11], where

$$C_l = (1 - \alpha) C_l^{\text{ad}} + \alpha C_l^{\text{iso}} + 2\beta \sqrt{\alpha(1 - \alpha)} C_l^{\text{corr}}. \quad (3)$$

The two notations are related by

$$\alpha = B^2/(1 + B^2), \quad \beta = \cos \Delta. \quad (4)$$

Here the parameter α runs from purely adiabatic ($\alpha = 0$) to purely isocurvature ($\alpha = 1$), while β defines the correlation coefficient, with $\beta = +1/-1$ corresponding to maximally correlated/anticorrelated modes. This notation has the advantage that the full parameter space of $(\alpha, 2\beta\sqrt{\alpha(1 - \alpha)})$ is contained within a circle of radius 1/2. The North and South rims correspond to fully correlated ($\beta = +1$) and fully anticorrelated ($\beta = -1$) perturbations, with the equator corresponding to uncorrelated perturbations ($\beta = 0$). The East and West correspond to purely isocurvature and purely adiabatic perturbations, respectively. Any other point within the circle is an arbitrary admixture of adiabatic and isocurvature modes.

In order to compute the theoretical prediction for the C_l coefficients of the temperature and polarization power spectra, as well as the matter spectra $P(k)$, for all four different components, we have used a CMB code developed by one of us (A.R.) which coincides, within 2% errors, with the values provided by CMBFAST for AD and CDI modes, and also includes the neutrino isocurvature modes as well as the cross-correlated power spectra. Note that the code defines the tilt of each power spectrum with respect to a pivot scale k_0 corresponding the present value of the Hubble radius, while CMBFAST uses $k_0 = 0.05 \text{ Mpc}^{-1}$: so, the comparison of our results with those of Refs. [8] for the CDI mixed model is not straightforward.

TABLE I: The one-dimensional 2σ ranges on the isocurvature mode coefficients for the various models, uncorrelated (middle column) and correlated (right column).

model	α	α	$2\beta [\alpha(1 - \alpha)]^{1/2}$
CDI	< 0.31	< 0.47	$-0.31 \text{ to } 0.31$
BI	< 0.91	< 0.95	$-0.80 \text{ to } 1.00$
NID	< 0.76	< 0.77	$-0.30 \text{ to } 0.78$
NIV	< 0.60	< 0.60	$-0.77 \text{ to } 0.35$

Results. We now describe the different bounds for each specific mode. See Table I for a summary.

CDM isocurvature. Assuming no correlation between the adiabatic and CDM isocurvature modes, we find an upper bound $\alpha < 0.31$ at 95% c.l. on the isocurvature fraction, see Table I. The probability distribution for α is given in Fig. 1a. The best-fit model parameters are listed in Table II, and the corresponding power spectra are shown in Fig. 2 (left plots). The deviation from a pure adiabatic model does *not* improve the goodness-of-fit, since the minimum χ^2 value goes from 1478.8 to 1478.3, while the number of degrees of freedom decreases from 1435 to 1433. The situation does not change significantly when we include a possible correlation: the minimum χ^2 is still around 1478.0, and the individual 2σ bounds on the coefficients read $\alpha < 0.47$ and $-0.31 < 2\beta\sqrt{\alpha(1 - \alpha)} < 0.31$ at 95% c.l., while the joint probability contours on (α, β) are shown in Fig. 1b. Most of the constraints on this model come from the WMAP TT power spectrum. For comparison, we repeated our analysis replacing WMAP and ACBAR by the Wang et

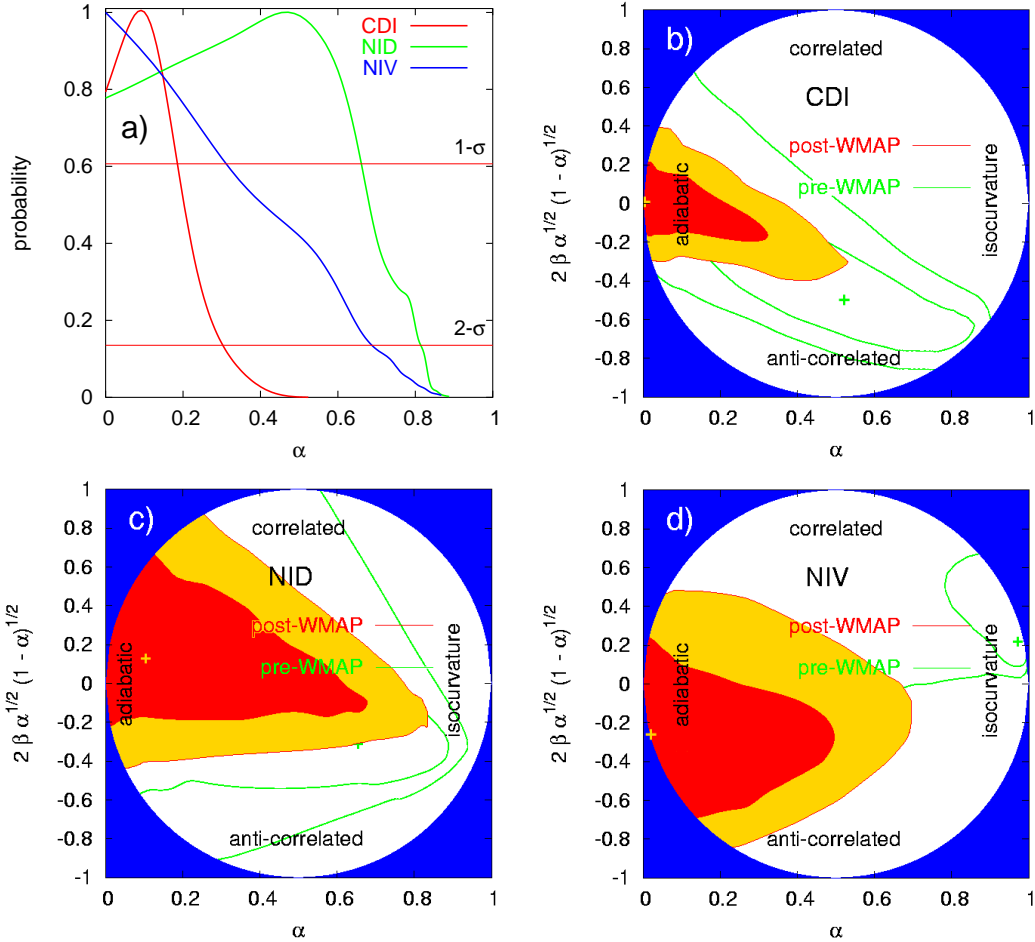


FIG. 1: a) the likelihood function of the isocurvature fraction α , for three different types of uncorrelated isocurvature modes (i.e., with the prior $\beta = 0$); b) the 1 and 2σ contours of α and the cross-correlated mode coefficient $2\beta\sqrt{\alpha(1 - \alpha)}$, for the CDM isocurvature mode: the small (red) contours are based on all the data, with one flat prior $n_{\text{iso}} > 0.6$, while the large (green) ones show the situation before WMAP, with an additional prior $\omega_B < 0.037$; c) same as b) for NID; d) same as b) for NIV. The marginalization is approximated by a maximum likelihood fit of the other parameters for each pair of values (α, β) .

al. [16] CMB data compilation, which includes all the pre-WMAP CMB temperature data. In that case, the results exhibit a wide parameter degeneracy (as indicated by previous studies [12, 13]), and a large fraction of anti-correlated isocurvature modes cannot be excluded, up to $(\alpha, \beta) = (0.9, -1)$, provided one allows for a very large baryon fraction. Therefore, we conclude that the WMAP TT data is very powerful in constraining the isocurvature fraction. On the other hand, we checked explicitly that the effect of the WMAP TE power spectrum is not very strong with respect to that of TT (possibly because of the relatively larger error bars, see Fig. 2).

In the curvaton scenario, the case in which the CDM is created before the curvaton decay while the curvature perturbations are small, corresponding to $(\alpha, \beta) = (0.9, -1)$ in our notation (3), is completely excluded, as already emphasized in Ref. [7, 14]. The case in which the CDM is created by the decay of the curvaton leads to $\beta = 1$; with such a prior, we obtain a sharp 2σ

bound: $\alpha < 0.04$ or, in the notation of Ref. [13], $B < 0.2$ (the authors of Ref. [14] obtain a more restrictive bound $B < 0.43$ $\Omega_B/\Omega_M \sim 0.1$, presumably because they use the curvaton-motivated assumption $n_{\text{iso}} = n_{\text{ad}}$).

Baryon isocurvature. The case of baryon isocurvature modes is qualitatively similar to that of CDI modes, since the spectra are simply rescaled by a factor $\Omega_B^2/\Omega_{\text{cdm}}^2$ ($\Omega_B/\Omega_{\text{cdm}}$) for the isocurvature power (cross-correlation) components: thus, significantly larger values of α will be allowed in the baryon case. Some approximate results for the BI modes could be deduced from the CDI results by an overall rescaling of the α parameter. However, we performed an exact analysis, and found the following bounds: $\alpha < 0.91$ (uncorrelated case), or $\alpha < 0.95$ and $-0.8 < 2\beta\sqrt{\alpha(1 - \alpha)} < 1$ (correlated case). In each case, the minimum χ^2 is, by definition, the same as for the CDI case. We provide the best-fit parameters in Table I, but for brevity we do not show this case in the figures.

In the curvaton scenario, the case in which the baryon

TABLE II: The best fit values of the parameters for the adiabatic (AD), uncorrelated (CDI, etc.), and correlated (c-CDI, etc.) isocurvature models, with the corresponding χ^2 and number of degrees of freedom ν . For the NIV uncorrelated model, the best-fit occurs for $\alpha = 0$ (i.e., purely adiabatic).

model	ω_B	ω_{cdm}	Ω_Λ	n_{ad}	n_{iso}	α	β	χ^2/ν
AD	0.021	0.12	0.70	0.95	—	—	—	1478.8/1435
CDI	0.023	0.12	0.73	0.99	1.02	0.10	—	1478.3/1433
BI	0.023	0.12	0.73	0.99	1.02	0.72	—	1478.3/1433
NID	0.023	0.12	0.73	0.99	0.95	0.37	—	1478.2/1433
NIV	0.021	0.12	0.70	0.95	—	0	—	1478.8/1433
c-CDI	0.022	0.12	0.71	0.97	1.23	0.01	1	1478.0/1432
c-BI	0.022	0.12	0.71	0.97	1.23	0.30	1	1478.0/1432
c-NID	0.022	0.12	0.73	0.97	1.04	0.10	0.26	1477.7/1432
c-NIV	0.021	0.12	0.71	0.95	0.71	0.03	-1	1477.5/1432

number is created before the curvaton decay while the curvature perturbations are small, corresponding to $(\alpha, \beta) = (0.9, -1)$, is also excluded at several σ 's, as previously found by in Ref. [14]. The case in which the baryon number is created by the decay of the curvaton predicts $\beta = 1$; we then find $\alpha < 0.5$, or $B < 1$ (again, our bound is more conservative than that of Ref. [14], which focused on the curvaton prediction $n_{\text{ad}} = n_{\text{iso}}$).

Neutrino density isocurvature. The 2σ bound for the uncorrelated case is $\alpha < 0.76$, while for the correlated adiabatic and neutrino mode we obtain $\alpha < 0.77$ and $-0.30 < 2\beta\sqrt{\alpha(1-\alpha)} < 0.78$. The likelihood contours in the (α, β) plane are shown on Fig. 1. The best-fitting models for the two cases – given in Table II and plotted in Fig. 2 (right plots) – are still extremely close to the adiabatic model, leading to no significant improvement in the likelihood, $\Delta\chi^2 = 0.6$ vs. $\Delta\chi^2 = 1.1$, respectively. Note that with the pre-WMAP CMB data plus the 2dFGRS power spectrum, significantly larger fractions, up to $(\alpha, \beta) = (0.9, -0.6)$, of correlated NID modes were then

allowed, but are now excluded with great confidence.

The authors of Ref. [7] discuss an interesting mechanism under which the curvaton could generate some fully correlated or anticorrelated NID modes, through inhomogeneities in the neutrino/antineutrino asymmetry parameter. However, our bounds for these cases are very restrictive, $\alpha < 0.18$ (correlated), or $\alpha < 0.02$ (anticorrelated). In the notation of Ref. [13], this is equivalent to $B < 0.47$ or $B < 0.14$, respectively.

Neutrino velocity isocurvature. Our results for these perturbations are summarized by $\alpha < 0.60$ at 95% c.l., for the uncorrelated case, see Table I, and $\alpha < 0.60$ with $-0.77 < 2\beta\sqrt{\alpha(1-\alpha)} < 0.35$ for the correlated case. The likelihood contours in the (α, β) plane are shown on Fig. 1. The best-fitting model for each case is given in Table II. Again, the presence of such a mode is not significantly favored: in the uncorrelated case, the best-fitting model is still the pure adiabatic one ($\alpha = 0$), while in the correlated case the χ^2 improvement is only $\Delta\chi^2 = 1.3$. The impact of WMAP on these bounds is again spectacular. Using only the pre-WMAP CMB data compilation and the 2dFGRS power spectrum, we find that half of the parameter space (with $0 < \alpha < 1$ and $0 < \beta < 1$) was allowed until recently (at the expense of an unnaturally high baryon fraction and scalar tilt).

Conclusions. Using the recent measurements of temperature and polarization anisotropies in the CMB by WMAP, as well as the matter power spectrum measured by 2dFGRS, we obtained very stringent bounds on a possible isocurvature component in the primordial spectrum of density and velocity fluctuations. We have considered both correlated and uncorrelated adiabatic and isocurvature modes, and put strong constraints on the curvaton scenario of primordial perturbations.

Acknowledgements. This work was supported in part by a CICYT project FPA2000-980.

[1] A. D. Linde, Phys. Lett. B **158**, 375 (1985); L. A. Kofman and A. D. Linde, Nucl. Phys. B **282**, 555 (1987); S. Mollerach, Phys. Lett. B **242**, 158 (1990); A. D. Linde and V. Mukhanov, Phys. Rev. D **56**, 535 (1997); M. Kawasaki, N. Sugiyama and T. Yanagida, Phys. Rev. D **54**, 2442 (1996); P. J. E. Peebles, Astrophys. J. **510**, 523 (1999).
[2] D. Polarski and A. A. Starobinsky, Phys. Rev. D **50**, 6123 (1994); M. Sasaki and E. D. Stewart, Prog. Theor. Phys. **95**, 71 (1996); J. García-Bellido and D. Wands, Phys. Rev. D **53**, 5437 (1996); M. Sasaki and T. Tanaka, Prog. Theor. Phys. **99**, 763 (1998).
[3] C. Gordon, D. Wands, B. A. Bassett and R. Maartens, Phys. Rev. D **63**, 023506 (2001); N. Bartolo, S. Matarrese and A. Riotto, Phys. Rev. D **64**, 123504 (2001); D. Wands, N. Bartolo, S. Matarrese and A. Riotto, Phys. Rev. D **66**, 043520 (2002); F. Di Marco, F. Finelli and R. Brandenberger, Phys. Rev. D **67**, 063512 (2003).
[4] D. Langlois, Phys. Rev. D **59**, 123512 (1999); D. Langlois and A. Riazuelo, Phys. Rev. D **62**, 043504 (2000).
[5] G. Efstathiou and J. R. Bond, Mon. Not. R. Astron. Soc. A **218**, 103 (1986); **227**, 33 (1987); P. J. E. Peebles, Nature **327**, 210 (1987). H. Kodama and M. Sasaki, Int. J. Mod. Phys. A **1**, 265 (1986); **2**, 491 (1987); S. Mollerach, Phys. Rev. D **42**, 313 (1990).
[6] M. Bucher, K. Moodley and N. Turok, Phys. Rev. D **62**, 083508 (2000); Phys. Rev. Lett. **87**, 191301 (2001).
[7] D. H. Lyth and D. Wands, Phys. Lett. B **524**, 5 (2002); D. H. Lyth, C. Ungarelli and D. Wands, Phys. Rev. D **67**, 023503 (2003).
[8] C. L. Bennett *et al.* [The WMAP Collaboration], astro-ph/0302207; L. Page *et al.*, astro-ph/0302220; H. V. Peiris *et al.*, astro-ph/0302225.
[9] C. L. Kuo *et al.* [The ACBAR Collaboration], astro-ph/0212289; J. H. Goldstein *et al.*, astro-ph/0212517.
[10] J. A. Peacock *et al.* [The 2dFGRS Collaboration], Nature **410**, 169 (2001); W. J. Percival *et al.*, Mon. Not. R.

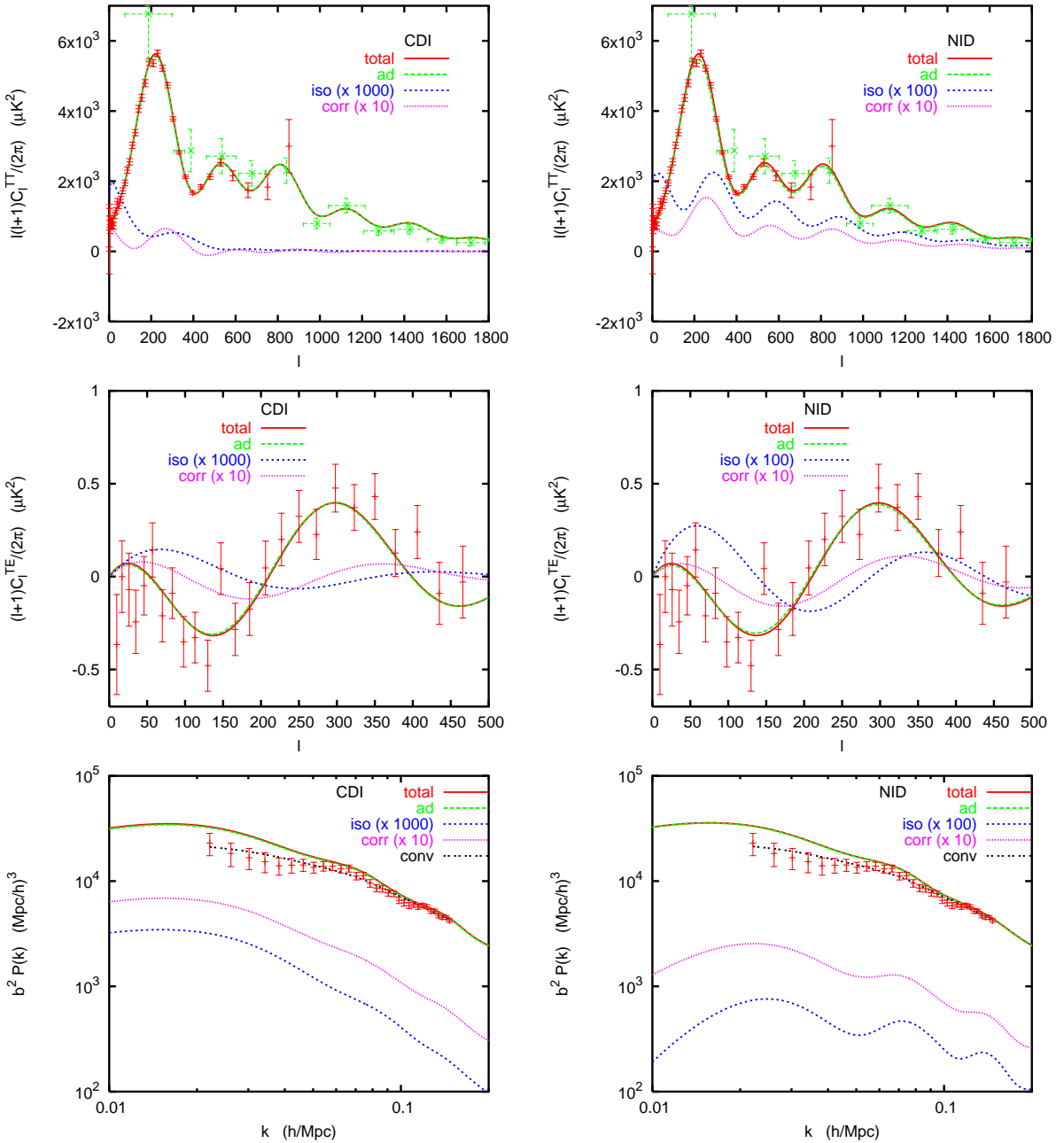


FIG. 2: Some best fit models compared to data. The left plots correspond to correlated CDM isocurvature modes, the right plots to neutrino density isocurvature modes. The parameters of these models can be seen in Table II. From top to bottom, we show the C_l^{TT} , C_l^{TE} and $P(k)$ power spectra, as well as the contribution of each component: adiabatic (ad), isocurvature (iso), cross-correlated (corr). The last two components have been rescaled by a factor indicated in each figure. We also show the data points that we use throughout the analysis, from WMAP, ACBAR and 2dF. In the case of the matter power spectrum, we plot in addition the theoretical spectrum convolved with the experimental window function (conv), in order to allow for a visual comparison with the data (which is not possible directly with the unconvolved power spectrum, due to the shape of the window functions). Note that these two best-fit models are extremely close to the pure adiabatic one: the differences in the respective power spectra would be indistinguishable by eye.

Astron. Soc. A **327**, 1297 (2001); **337**, 1068 (2002).

[11] R. Stompor, A. J. Banday and K. M. Gorski, *Astrophys. J.* **463**, 8 (1996); P. J. E. Peebles, *Astrophys. J.* **510**, 531 (1999); E. Pierpaoli, J. García-Bellido and S. Borgani, *JHEP* **9910**, 015 (1999); M. Kawasaki and F. Takahashi,

Phys. Lett. B **516**, 388 (2001); K. Enqvist, H. Kurki-Suonio and J. Välimäki, *Phys. Rev. D* **62**, 103003 (2000); **65**, 043002 (2002).

[12] R. Trotta, A. Riazuelo and R. Durrer, *Phys. Rev. Lett.* **87**, 231301 (2001); *Phys. Rev. D* **67**, 063520 (2003).

- [13] L. Amendola, C. Gordon, D. Wands and M. Sasaki, Phys. Rev. Lett. **88**, 211302 (2002).
- [14] C. Gordon and A. Lewis, astro-ph/0212248.
- [15] J. Välimäki and V. Muhonen, astro-ph/0304175.
- [16] This data compilation is available online on Max

Tegmark's website, <http://www.hep.upenn.edu/~max/cmbllsllens.html>. More details on a previous version are given in X. Wang, M. Tegmark, B. Jain and M. Zaldarriaga, astro-ph/0212417.